THE AMERICAN SOCIETY OF MECHANICAL ENGINEERS
345 E. 47 St., New York, N.Y. 10017

86-GT-234

Influence of Free Stream Turbulence and Blade Pressure Gradient on Boundary Layer and Loss Behaviour of Turbine Cascades

H. HOHEISEL
R. KIOCK

Deutsche Forschungs- und Versuchsanstalt
für Luft- und Raumfahrt (DFVLR),
Institut für Entwurfsaerodynamik
Braunschweig, Germany

H. J. LICHTFUß
Motoren- und Turbinen- Union GmbH (MTU)
München, Germany

L. FOTTNER
Universität der Bundeswehr München
Institut für Strahlantriebe
Neubiberg, Germany

ABSTRACT

The optimization of the blade surface velocity distribution is promising a reduction of turbine cascade losses. Theoretical and experimental investigations on three turbine cascades with the same blade loading show the important influence of the blade pressure gradient and the free stream turbulence on the loss behaviour. The results presented demonstrate that it is the boundary layer transition behaviour that determines the losses on turbine cascades. An enormous effort in measuring technique is required in order to define the location of transition from cascade experiments very accurately.

NOMENCLATURE

c	chord
c_{p2}	pressure distribution coefficient, based on exit conditions, see eq. (8)
e	standard location of traverse plane
e_{rms}	root mean square a-c CTA (Constant Temperature Anemometer) output voltage
E	mean CTA output voltage, with flow
H_{12}	shape factor, $H_{12} = \delta_1/\delta_2$
H_{43}	shape factor, $H_{43} = \delta_4/\delta_3$
Ma_{2th}	isentropic exit Mach number, $Ma_{2th} = f(p_K/p_{o1})$
p	static pressure
p_o	total pressure
q	dynamic head, $q = p_o - p$
Re_2	Reynolds number based on blade chord and exit conditions, $Re_2 = w_2 \cdot c/\nu_2$
s	blade pitch (spacing)
Tu_1	degree of turbulence at cascade inlet, $Tu_1 = \sqrt{\overline{w_1'^2}}/w_1$
w	flow velocity
x, y	profile coordinates, bitangential
β	flow angle, see fig. 3
β_S	stagger angle, see fig. 3
δ	boundary layer thickness
$\delta_1, \delta_2, \delta_3, \delta_4$	displacement, momentum, energy, and density thickness
η	coordinate normal to blade surface
ζ_{V2}	total pressure loss coefficient, see eq. (7)
ν	kinematic viscosity
ρ	density
τ	shear stress

Subscripts, Abbreviations

1	cascade inlet plane
2	cascade exit plane, homogeneous flow
δ	edge of boundary layer
K	tank (cascade exit condition)
max	maximum
th	theoretical isentropic flow
tr	trailing edge
R	reattachment
S	separation
T	transition onset
T M M	time marching method

INTRODUCTION

An important aspect of turbine aerodynamic design is the question of optimum profile shape to reduce the losses. With respect to the boundary layer state of actual turbomachinery blades, it is essential to find velocity distributions with the laminar-turbulent transition point as far downstream as possible. In particular, two factors affect the transition behaviour, namely the pressure gradient on the blade surface and the free stream turbulence. On the other hand, it is well known from turbine cascade experience, especially at low Reynolds numbers, that frequently laminar separation takes place before transition to the turbulent state is attained. Therefore the point at which this condition occurs, and the nature of transition are the object of several publications, e.g. Gostelow [1].

Presented at the International Gas Turbine Conference and Exhibit
Dusseldorf, West Germany—June 8-12, 1986

One of the first publications about the influence of turbulence on turbine cascade performance was given by Hebbel [2]. The importance of investigations on cascades under turbomachinery conditions was demonstrated by Kiock [3], [4] and by Pfeil and Pache [5]. Abu-Ghannam and Shaw [6] investigated natural transition with pressure gradient and turbulence for a flat plate flow. They recommended to consider the curvature too. Current turbine velocity distributions were simulated by Sharma et al. [7] to study the transitional boundary layer. The boundary layer behaviour with respect to heat transfer is the object of the work by Blair [8] and by Rued and Wittig [9]. In general, no method is available which will predict reliably the influence of parameters like pressure gradient and turbulence on the blade boundary layer behaviour. As conclusion from a Symposium on Transition in Turbines held recently at the NASA Lewis Research Center a collection of existing transition data should be provided as standard cases against which other models could be tested, see Gaugler [10].

The references quoted constitute only a selection. In spite of a large number of publications there is little information available about the influence of actual turbulence level on turbine blading performance. The present investigations describe the boundary layer and loss behaviour of three turbine cascades of different geometries but with the same loading. Applying a current boundary layer integral calculation method, the influence of different blade velocity distributions and free stream turbulence levels on the cascade performance was predicted. Experiments, performed in the High Speed Cascade Wind Tunnel of DFVLR Braunschweig, support these theoretical results.

THEORETICAL INVESTIGATION

Cascade Design

To describe the complicated flow behaviour of an axial turbine the "quasi-3D design" has been applied. First the axial and radial velocity distributions are calculated, followed by several blade-to-blade computations through cascades in order to obtain also the corresponding circumferential distribution of the velocity. The object of the blading design is to find an adequate profile shape to verify the velocity triangle with respect to minimal losses. It is necessary also to incorporate some strong mechanical and turbine cooling constraints [11]. These additional design parameters may be the reason that there is no systematic family for turbine profiles as is the case for compressors (e. g. NACA 65 or C4 profiles). Therefore, the turbine profile design is an individual process to be performed in an iterative manner.

The geometric design of the profiles presented in this paper was performed in the traditional manner of superimposing a thickness distribution on a camber line. The camber line is defined by two polynomials of a maximum order of four which are patched to each other at a selected connection point in such a way that the slope remains. Superimposed to the camber line then is a thickness distribution of a similar mathematical character than that of the camber line, starting on the leading edge circle or ellipse at a prescribed wedge angle and ending on the trailing edge circle at another wedge angle. Performing an inviscid blade-to-blade flow calculation then yields pressure or velocity distributions along the pressure and suction surfaces of the profile which serve as a measure of the attained aerodynamic quality (direct method).

Another design procedure which is now available to create the blade shape is the inverse or design method. A very versatile method of this type is given by E. Schmidt [12] using a compressible inviscid flow model.

Both blading design methods use the profile velocity distribution as a criterion for the aerodynamic quality of the design, i.e. they take into account the close connection between the profile losses (due to blade boundary layer) and the blade surface velocity distribution. Thus, the velocity distribution being input for these methods has to be optimized with respect to low losses of the blading. Since turbine cascades have to accelerate the flow from inlet to outlet, their profile velocity distribution could have in principle a shape without any deceleration region, as shown in figure 1. In practical applications this "ideal" distribution will be changed more or less, especially with respect to the above mentioned mechanical constraints and because of alterations necessary to obtain more desirable boundary layer characteristics.

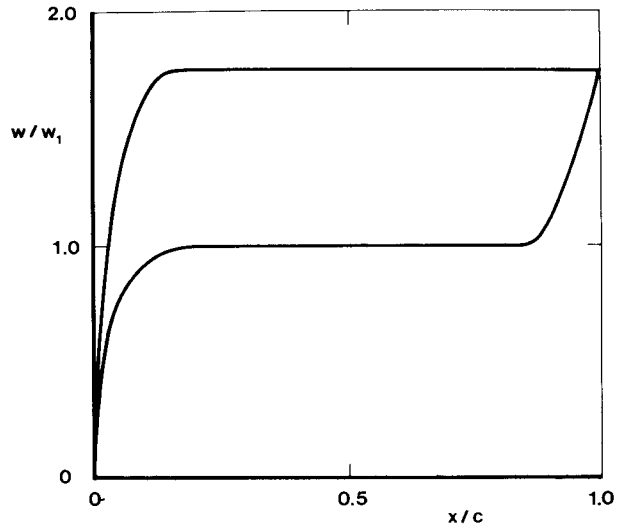

Figure 1: "Ideal" velocity distribution for accelerating cascades

Experience on several turbine cascades at design conditions shows a mixed laminar-turbulent boundary layer on the suction surface and a mostly laminar boundary layer on the pressure surface. It is therefore necessary to primarily optimize the velocity distribution on the suction surface with respect to low losses. The laminar boundary layer should be maintained as far downstream as possible. Transition is required to take place without forming a laminar separation bubble. The extent of a rearward deceleration has to be carefully limited to avoid flow separation in this region. In order to obtain information about an optimal velocity distribution on the suction surface considering

the boundary layer state, three cascades with different velocity distributions but the same aerodynamic loading were designed for a typical LP turbine condition. These velocity distributions are shown in, figure 2. The chosen velocity distributions designated by T104, T105 and T106, can be described as follows:

- Type T104 is front-loaded with an almost uniform suction side velocity, incorporating a small amount of deceleration in the rear part.
- Types T105 and T106 are aft-loaded, showing an acceleration on the suction side over the front part with a maximum velocity at approximately 50 % chord followed by a deceleration to the outlet velocity. The types T105 and T106 differ only in their peak velocity resulting in different pressure gradients over the rear part of the suction side. The velocity distribution along the pressure side remains nearly unchanged for these cases.

The associated profile shapes and cascade geometries are shown in figure 3. These cascades were designed by the direct method.

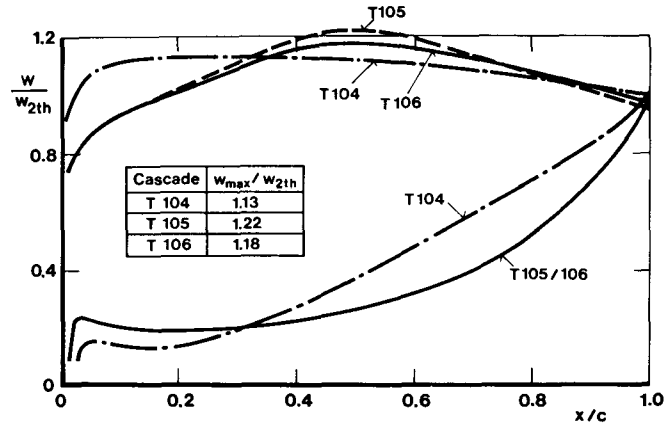

Figure 2: Design velocity distribution

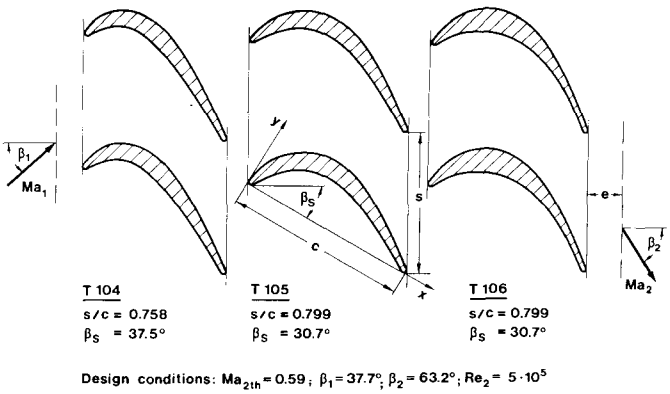

Figure 3: Cascade geometry and nomenclature

Boundary Layer Behaviour of Different Types of Velocity Distributions

For an assessment of the boundary layer behaviour subject to the three velocity distributions, a boundary layer integral method was applied. Starting from Prandtl's boundary layer equations for two-dimensional flow expressing the conservation laws of mass (continuity equation) and of momentum

$$\rho u \frac{\partial u}{\partial x} + \rho v \frac{\partial u}{\partial y} = - \frac{\partial p}{\partial x} + \frac{\partial \tau}{\partial y} \qquad (1)$$

with a usual assumption on the shear stress τ, integration of eq. (1) leads to the compressible integral equation of momentum

$$\frac{d\delta_2}{dx} + \frac{\delta_2}{w_\delta} \cdot \frac{dw_\delta}{dx} \left[2 + H_{12} - Ma_\delta^2 \right] - \frac{\tau_w}{\rho_\delta \cdot w_\delta^2} = 0 \qquad (2)$$

and the compressible integral equation of mechanical energy

$$\frac{d\delta_3}{dx} + \frac{\delta_3}{w_\delta} \frac{dw_\delta}{dx} \left[3 + 2H_{43} - Ma_\delta^2 \right] - \frac{2}{\rho_\delta \cdot w_\delta^3} \int_0^{w_\delta} \tau \cdot dw = 0 \qquad (3)$$

as given by Walz [13] in more detail. In the present paper two different transition criteria are taken into consideration:

- The criterion by Granville [14] describes the influence of turbulence intensity for flat plate flow and flow with pressure gradient at a low free stream turbulence level.
- An empirical criterion by Seyb [15], analytically given by Dunham [16], describes transition to be dependent on the following three parameters:

pressure gradient $$\lambda = \frac{\delta_2^2}{\nu} \cdot \frac{dw_\delta}{dx} \qquad (4)$$

momentum thickness Reynolds number $$Re_{\delta 2} = \frac{w_\delta \cdot \delta_2}{\nu} \qquad (5)$$

local turbulence level $$Tu = \frac{\sqrt{\overline{w'^2}}}{w_\delta} \qquad (6)$$

This definition of the degree of turbulence takes into account the local acceleration/deceleration in the blade channel and thus differs from the inlet free stream value.

At the design condition laminar separation is assumed to be absent or of small extent. For this condition figure 4 shows the related momentum thickness versus chord of the three cascades at the low turbulence level of $Tu_1 = 0.8\%$ where the respective locations of transition (T) according to Granville's transition criterion are indicated by the arrows. At this low turbulence level the smallest value of the momentum thickness at the trailing edge is obtained by the type T104 as a result of the transition behaviour, and of the moderate deceleration over the rear part of the blade surface. The stronger aftward pressure gradient of T105 causes earlier transition which leads to a larger momentum thickness in the trailing edge region.

Looking at the transition behaviour by using the two criteria mentioned above, figure 5 shows the influence of the free stream turbulence on transition onset (T) for the three cascades investigated. With increasing

turbulence Dunham's criterion shows transition onset to be located considerably further upstream for all three cascades, whereas the Granville criterion shows a similar strong influence for the T104 type only.

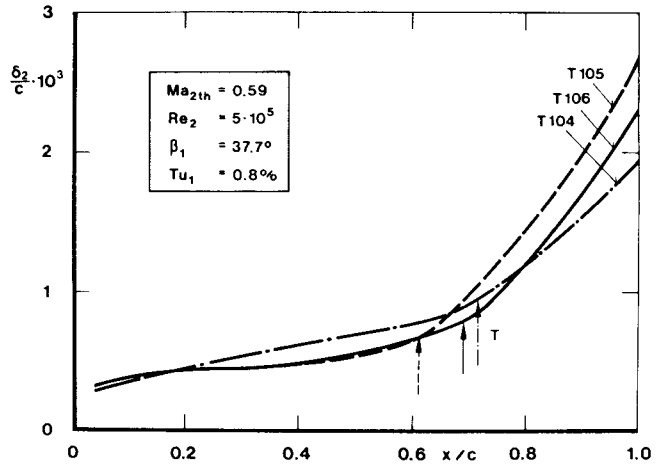

Figure 4: Calculated momentum thickness of suction surface with Granville's transition criterion

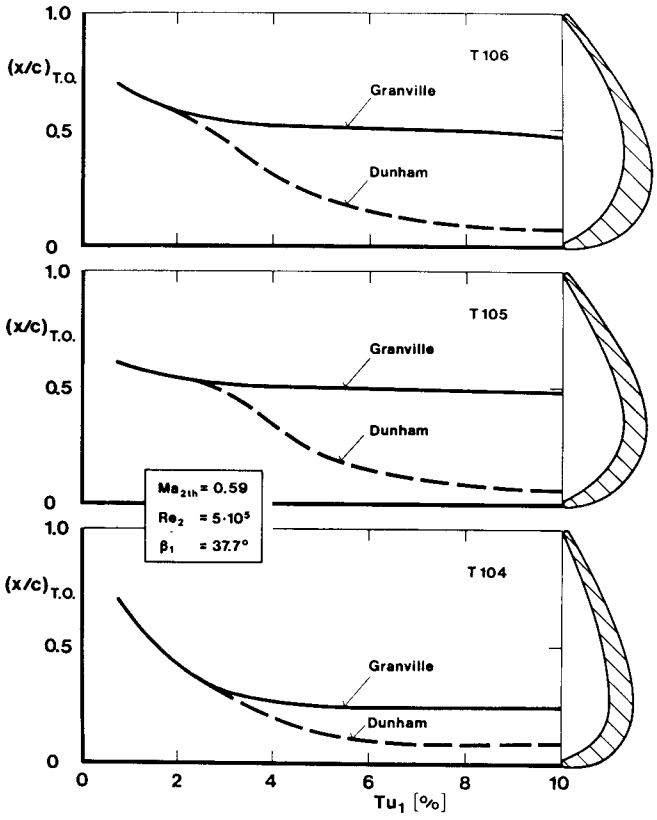

Figure 5: Influence of degree of turbulence on transition onset on the suction surface

Values of the momentum thickness at the trailing edge calculated by the integral boundary layer method are shown in figure 6, where the influence of deceleration attributed to the different cascade types is displayed with the turbulence intensity as parameter. As can be seen a dominant influence of the turbulence level on the trailing edge momentum thickness exists for each cascade type, of which only the front-loaded type T104 attains a low value of momentum thickness at low turbulence level. At actual turbulence levels for turbine cascades the T106 type seems to represent the best compromise between deceleration rate and peak velocity location when Granville's transition criterion is applied.

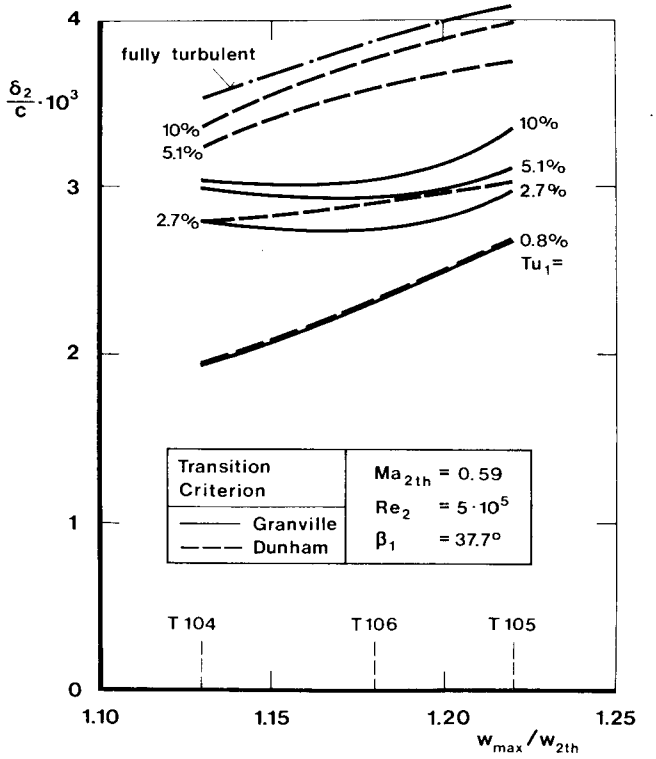

Figure 6: Effect of deceleration on the momentum thickness at the suction side trailing edge

EXPERIMENTAL INVESTIGATION

Apparatus and Test Programme

The experimental investigations were carried out in the High Speed Cascade Wind Tunnel of DFVLR at Braunschweig [17]. The tunnel was installed in a tank which could be evacuated from 1 to 0.05 bar. An independent variation of Mach number and Reynolds number was possible. The degree of turbulence was about Tu_1 = 1 %. It could be increased up to Tu_1 = 8 % using grids of crossed bars upstream of the cascade [18]. The tunnel had a test section width of h = 300 mm and an adjustable height of 250 to 500 mm depending on the inlet angle. Each cascade consisted of 7 blades of a chord length of c = 100 mm resulting in an aspect ratio of h/c = 3. No side wall suction was applied.

In general, the design point of the cascades only will be considered here: $\beta_1 = 37.7^{\circ}$; $Ma_{2th} = 0.59$; $Re_2 = 5 \cdot 10^5$.

Wake traverse measurements (total pressure, static pressure and outlet flow angle) were performed with a wedge type probe [17] located at 40 % of chord axially downstream of the blade trailing edge plane. Surface pressure distributions were measured using static pressure tappings on the suction and the pressure sides of the blades adjacent to the centre blade.

Boundary layer measurements were carried out at different positions of the blade suction surface by a flattened Pitot probe of 0.15 mm x 1.30 mm head size in order to obtain velocity profiles and integral quantities. The probe was calibrated for Mach and Reynolds number, flow angle and turbulence level. Corrections were applied from these calibrations on the basis of a comparison with flat plate experiments [19] and with measurements by a laser-Doppler anemometer respectively [20]. Another probe of 0.30 mm x 0.80 mm (also a flattened Pitot tube, called Preston type probe) was moved at a constant distance from the blade surface, $\eta = 0.15$ mm, in order to detect boundary layer transition. Details of this technique are described in [21]. Additional tests were performed also in order to detect boundary layer transition by flow visualization method and by the heated thin film technique.

Evaluation of the Experimental Data

The wake data were evaluated by transforming the non-homogeneous flow in the measuring plane into an equivalent homogeneous flow applying the laws of conservation, see [22]. This evaluation leads to the total pressure loss coefficient which is defined as

$$\zeta_{V2} = \frac{p_{o1} - p_{o2}}{p_{o1} - p_K} \qquad (7)$$

For the pressure distribution a non-dimensional coefficient is defined as

$$c_{p2} = \frac{p(x/c) - p_K}{p_{o1} - p_K} \qquad (8)$$

As an alternative the velocity ratio w/w_{2th} with $w = f(p/p_{o1})$ and $w_{2th} = f(p_K/p_{o1})$ may be used.

All boundary layer data were evaluated under the assumption of constant static pressure across the boundary layer. This leads to the standard definition, e.g. of the momentum thickness

$$\delta_2 = \int_0^{\delta} \frac{\rho(\eta)}{\rho_\infty} \cdot \frac{w(\eta)}{w_\infty} \left[1 - \frac{w(\eta)}{w_\infty}\right] d\eta \qquad (9)$$

For the detection of boundary layer transition by a flattened Pitot probe (also called Preston type) the local dynamic head was evaluated by the Pitot pressure at $\eta = 0.15$ mm and by the local surface static pressure which gives the ratio

$$\frac{q\ (x/c\ \eta)}{q\ (x/c)} = \frac{p_o\ (x/c,\eta) - p(x/c)}{p_{o1} - p(x/c)} \qquad (10)$$

The degree of turbulence in the inlet plane is defined as

$$Tu_1 = \frac{\sqrt{\overline{w_1'^2}}}{w_1} \qquad (11)$$

where w_1' is the fluctuating velocity component in the direction of w_1 obtained from a single hot-wire probe placed normal to the free stream velocity.

RESULTS AND DISCUSSION

Measured Pressure Distribution and Comparison with Theory

Figure 7 shows the measured and the calculated velocity distribution of the cascades T104 and T106. The theoretical results were obtained using Lehthaus's time-marching method [23]. From the experiments a case with the relatively high Reynolds number, $Re_2 = 9 \cdot 10^5$, was chosen in order to keep the influence of laminar separation bubbles low. Very good agreement between the calculated and the measured velocity distributions can be seen to exist for the two different types of turbine cascades. This gives confidence in the cascade design method used. Any differences between theory and experiments in the results presented may therefore be interpreted as inadequacies in the boundary layer method used, and, in particular, in the transition criterion applied.

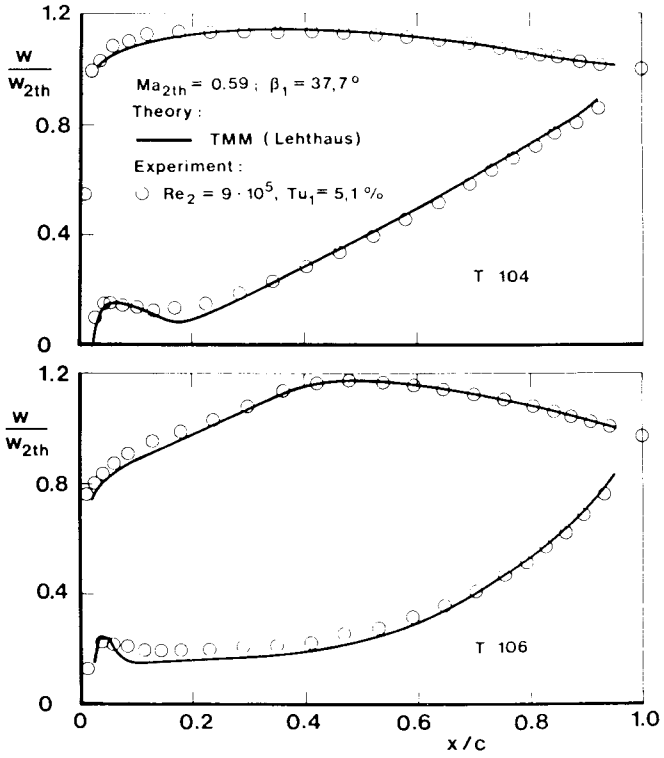

Figure 7: Blade velocity distribution, comparison of theory and experiment at design conditions

Boundary Layer Transition Location

The three cascades were investigated at Reynolds numbers of an actual turbine stage. In this Reynolds number range (Re_2=3 to 7 · 10^5)

laminar separation may occur [24]. Some results of the used measuring techniques are demonstrated and discussed.

Diagram (A) in figure 8 shows the pressure distributions on the suction surface of the cascades at the low turbulence level of Tu_1 = 0.8 %. Boundary layer transition from the laminar to the turbulent state via a separation bubble is indicated by the changing pressure gradients on the cascade types T105 and T106. The bubble starts, say, on T105 somewhat downstream of the suction peak at x/l = 0.6 as marked by S. Transition onset (T) occurs for this example at x/l = 0.75. The boundary layer reattaches at x/l = 0.80 (marked by R). On the cascade type T104, with the peak velocity in the front part, the different boundary layer states are not clearly determinable from the pressure plot. Other measuring techniques are necessary to clarify this question and will be discussed below. Diagram (B) in figure 8 shows the pressure distribution of T106 at different turbulence levels. With increasing turbulence level the detectable laminar separation bubble disappears almost completely.

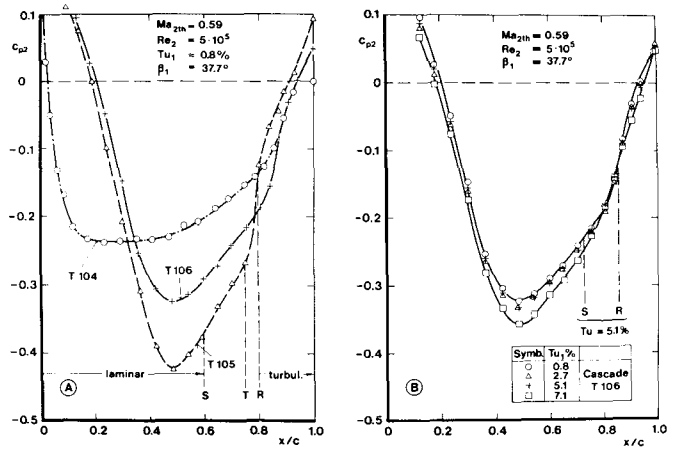

Figure 8: Pressure distributions on the suction surface (A) Influence of cascade type; (B) Influence of free stream turbulence on cascade T106

Another result concerning boundary layer transition is demonstrated in figure 9. Here, transition was detected by a Preston type probe. These results show the influence of the turbulence level on cascade T106. With increasing turbulence level the point of transition onset (T) is shifted upstream: All curves have a well defined minimum, indicating the start of transition as well as a well defined maximum, describing the completion of transition (R).

Measurements of the boundary layer velocity profile obtained for different values of the degree of turbulence are presented in figure 10 for T106. Velocity profiles w/w_δ are plotted at different locations x/c. These curves demonstrate the progressive change from laminar to "full" turbulent velocity profiles. This change in shape occurs between x/c = 0.75 and x/l = 0.95 which is in agreement with the pressure distributions (fig. 8) and with the Preston type probe results (fig. 9). This range thus defines the extent of a "laminar separated bubble" where a strong influence of the free stream turbulence is assumed to exist. On the other hand, from comparison with laser-Doppler measurements, it is known that in particular in the reverse flow zone the presence of probes alters the velocity distribution near the wall. This influence disappears with increasing distance of the probes from the surface [20]. These findings are of great importance when comparing test results with empirical correlations on laminar separation bubbles.

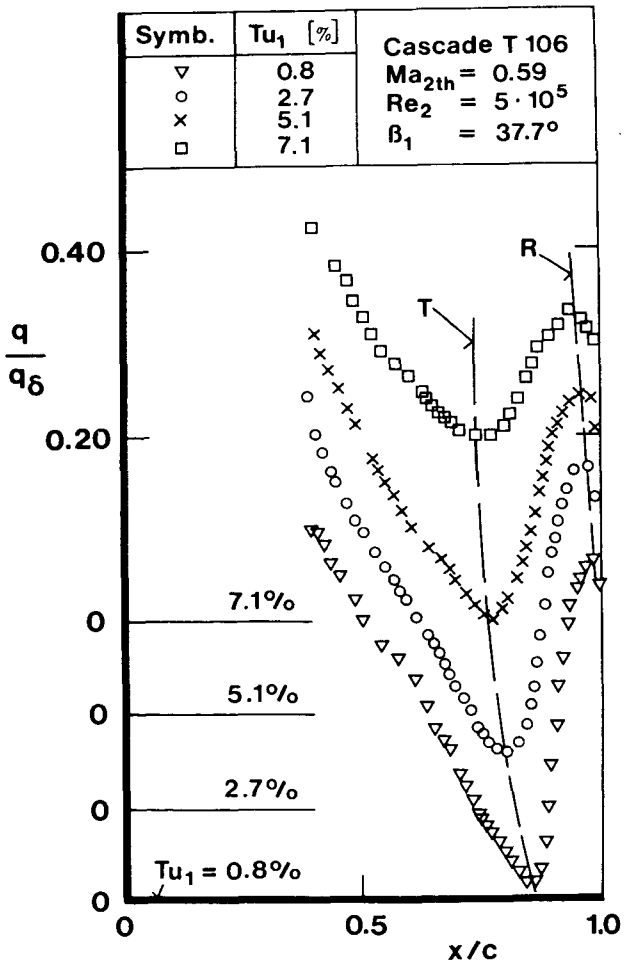

Figure 9: Boundary layer transition on the suction surface, using Preston type probe

From the measured boundary layer velocity profiles some integral values were determined. Plotted in figure 11 are the momentum thickness δ_2/c and the shape factor $H_{12} = \delta_1/\delta_2$ versus chord length x/c for the same condition as that used in figure 10. The experimental results are compared with theoretical results, obtained by Granville's criterion for transition at different degrees of turbulence between Tu_1 = 0.8 % and 7.1 %. For the front part of the blade surface, poor agreement is found for the momentum thickness. In this part the boundary layer thickness is very thin (less than 1 mm). Little is known about the accuracy of

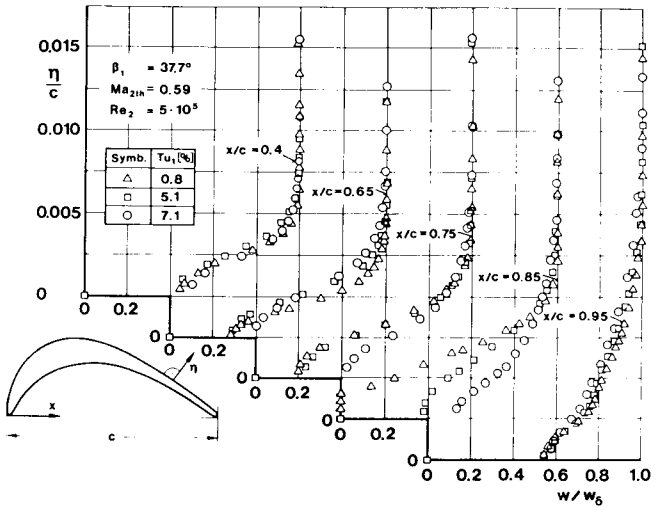

Figure 10: Boundary layer velocity profiles, suction surface, T106, influence of turbulence

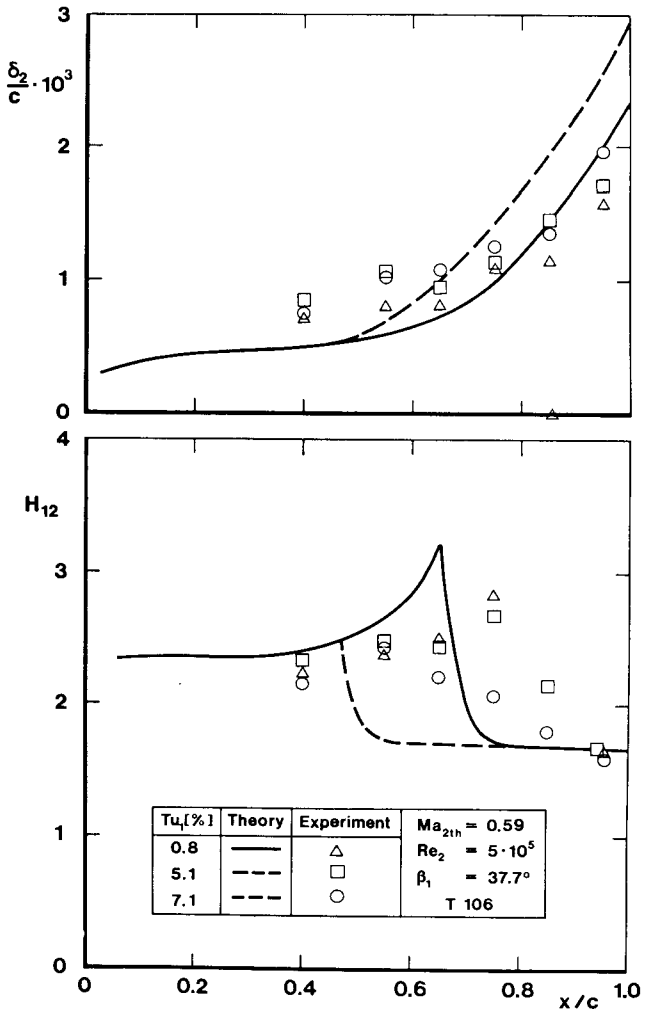

Figure 11: Integral values of the boundary layer, suction surface T106

measurements in boundary layers where the displacement thickness and the probe height are of the same order of magnitude. An error in measured momentum thickness of about $\Delta\delta_2/\delta_2 = \pm 14\,\%$ was found in our previous investigations [19]. For the rear part of the blade surface (i.e. downstream of transition) better agreement between theory and experiment is observed for the momentum thickness. An increase of δ_2 with the turbulence level is seen to exist as was to be expected.

A rather good agreement in the comparison of theory with experiment can also be observed concerning the shape factor H_{12} both for laminar and turbulent boundary layer conditions. The main difference is found in the location of transition (notable by the drop of H_{12}). The theoretical results indicate transition to take place further upstream than the experiments. Obviously, this is due to a deficiency of the transition criterion which does not determine the location and the extent of transition in the correct manner as yet [25].

A comparison of different measurement techniques for the detection of transition is shown in figure 12, i.e. curves from heated film technique, Preston type probe results, shape Factor H_{12} from boundary layer velocity profiles, and pressure distribution respectively. As to the thin film technique the distribution of the voltage coefficient e_{rms}/E versus x/c

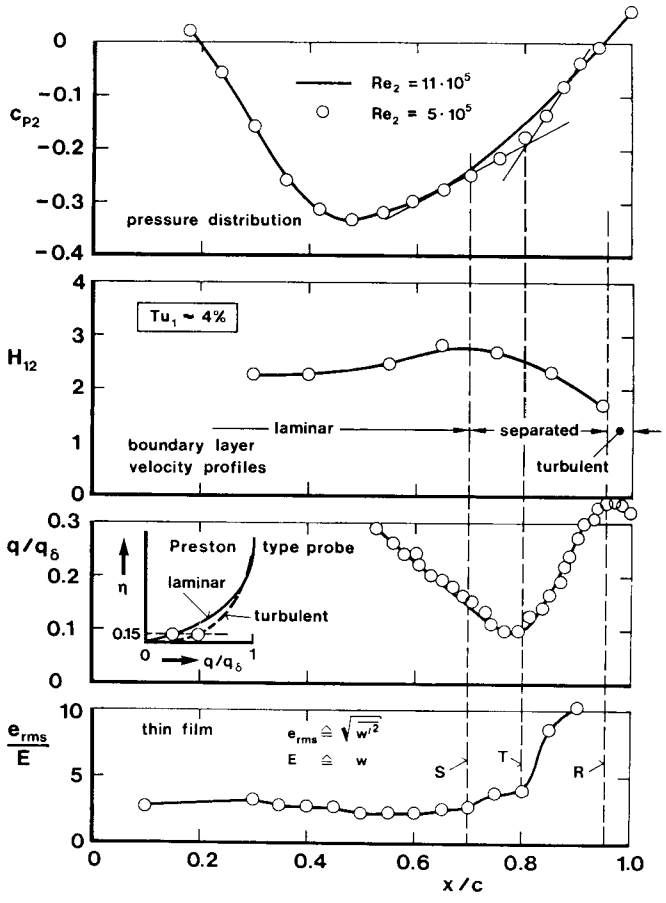

Figure 12: Determination of transition location from measurements

shows a first increase at x/c ≈ 0.7 which indicates the first change in heat transfer. At this location, the beginning of laminar separation (S) is also indicated by the appearance of turbulent spots detectable from the a - c signal on the oscilloscope screen (not shown here), from the pressure distribution, and from the maximum value of the shape factor. Transition onset (T) starts at x/c ≈ 0.8 indicated by the strong increase of e_{rms}/E. This location coincides with that of the minimum q/q_δ - value and with that of the change of the pressure gradient in the pressure distribution. The point of boundary layer reattachment (R) is defined by the maximum q/q_δ-value. These findings drawn from different measuring techniques give the confidence in the results on boundary layer transition.

The results for the extent of the boundary layer transition regime extracted from the experimental investigations of the three cascades are summarized in figure 13 and 14 in comparison with the theoretically determined transition using Granville's criterion. Figure 13 shows the influence of the Reynolds number at a constant turbulence level of about $Tu_1 \approx 5\,\%$, while figure 14 describes the effect of the turbulence level for two Reynolds numbers in the case of the cascade T106 only. These experimental results stem from:

- pressure distributions
- boundary layer velocity profiles
- Preston type probe measurements along the surface
- flow visualizations
- heated thin film technique (T104 and T106)

In general, the experimental results do not show "natural" transition as assumed in the theoretical investigations, but the "bubble"-type transition is found. A laminar separation bubble is closed by a turbulent reattachment. Start and extension of laminar separation are different depending on the pressure gradient of the three cascades. With increasing Reynolds number laminar separation is moving slightly upstream and the size of the bubbles decreases, which is also found in single airfoil investigation [26]. In the case of the front-loaded cascade type T104 and also for the aft-loaded type T105 with the stronger pressure gradient, transition starts in the same range x/c = 0.55 to 0.65. On the aft-loaded type T106 the "transition zone" begins more downstream than would be expected from the lower pressure gradient.

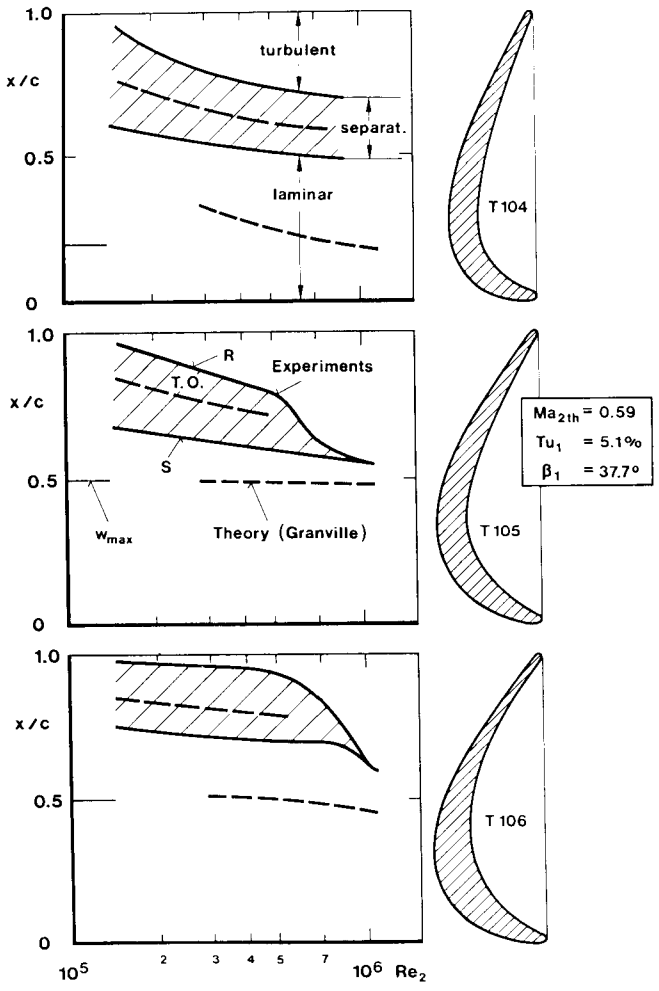

Figure 13: Effect of Reynolds number on transition location

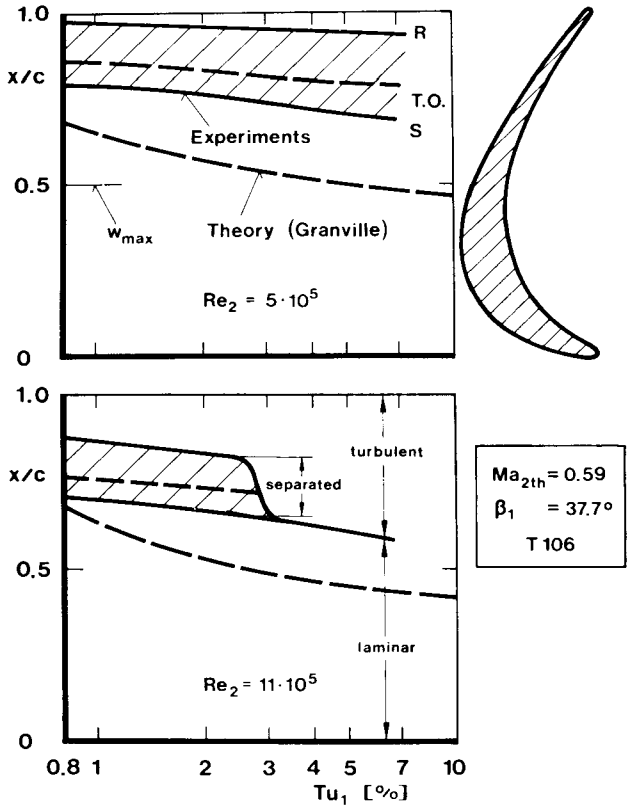

Figure 14: Effect of free stream turbulence on transition location, cascade T106

The influence of turbulence on the aft-loaded type T106 at the most important Reynolds number, $Re_2 = 5 \cdot 10^5$ (figure 14) shows only a

small change of transition onset and closure with increasing turbulence level. This experimentally determined behaviour is in agreement with the theoretical result, as shown earlier in figure 5, however, the locations x/c of theory and experiment differ strongly. At the higher Reynolds number, $Re_2 = 11 \cdot 10^5$, the laminar separation bubble disappears with increasing turbulence level. This behaviour is in agreement with the Granville criterion. However it should be noted that the present results are in disagreement with the correlation formula of Dunham, which was also found by Blair [8]. Therefore it seems to be necessary to study "natural" and "bubble"-induced transition in more detail in the future, but under the conditions of turbomachinery blades.

Boundary Layer Quantities

The different transition behaviour found for the three cascades is reflected in the momentum loss behaviour, too. Figure 15 shows the momentum thickness versus the flow deceleration (different types of cascade) near the trailing edge, i.e. at x/c = 0.95 at design conditions. At the low degree of turbulence $Tu_1 = 0.8\,\%$, the same experimental value of δ_2 is obtained for the front-loaded cascade T104 and for the aft-loaded cascade T106. The stronger pressure gradient of cascade T105 leads to higher loss in momentum. The comparison of experiment and theory shows rough agreement, both in level and in tendency. At the higher turbulence levels, a minimum momentum thickness is obtained for the aft-loaded cascade T106 which is qualitatively in agreement with the theoretical results. In view of the different transition mechanismes assumed for the theory and found in the experiments, no quantitative agreement could be expected.

The influence of Reynolds number on momentum thickness of the aft-loaded type T106 is shown in figure 16. At the low turbulence level

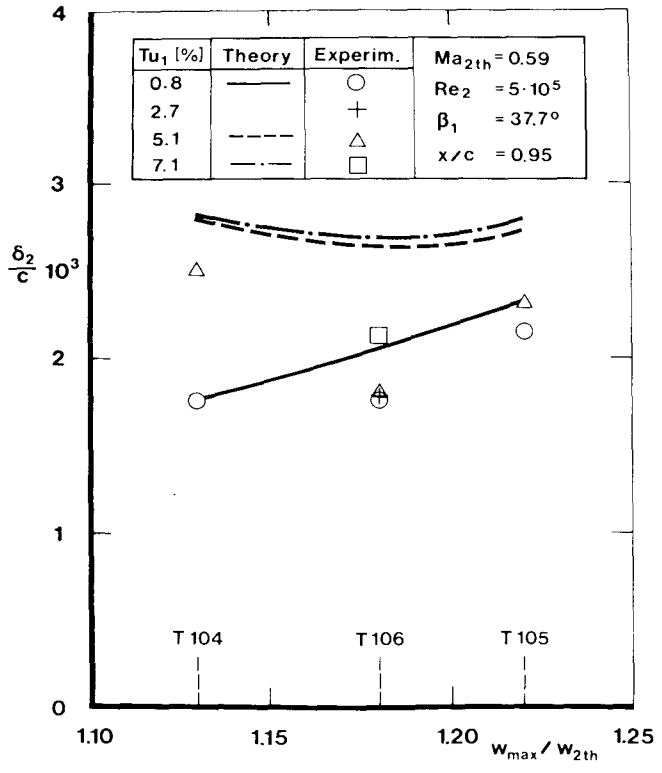

Figure 15: Effect of blade deceleration on momentum thickness, comparison between theory and experiment

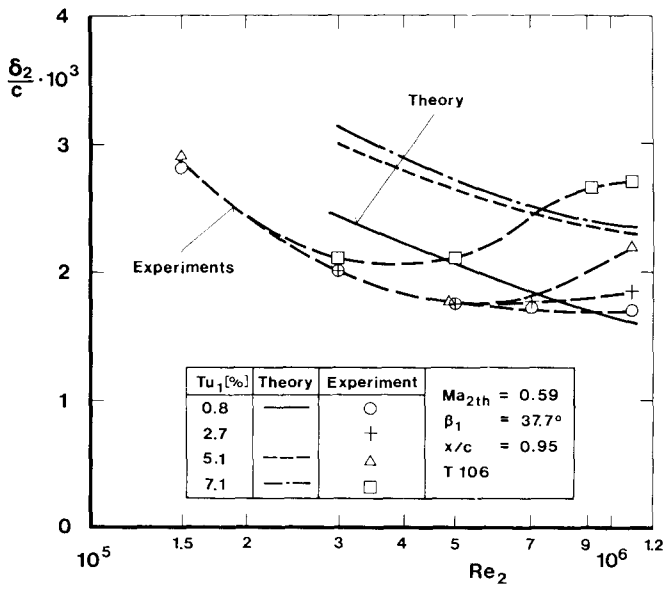

Figure 16: Effect of Reynolds number and free stream turbulence on momentum thickness, comparison between theory and experiment

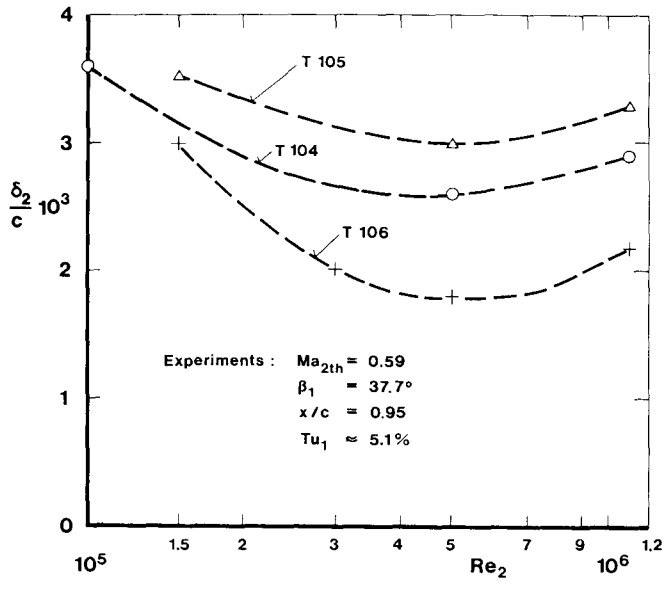

Figure 17: Effect of Reynolds number on momentum thickness, experiments on different cascades at constant turbulent level

of Tu_1 = 0.8 %, the Reynolds number has the dominant influence, as could be expected. At the higher turbulence levels the difference between experiments and theory can again be explained by the insufficient assumptions with regard to the transition criterion.

For the most important turbulence level of Tu_1 =5.1%, the momentum thickness of the three cascades, as obtained from experiments only, is plotted versus Reynolds number in figure 17. The minimum value of δ_2 at all three cascades occurs near the design Reynolds number, $Re_2 = 5 \cdot 10^5$. The aft-loaded cascade T106 with the moderate pressure gradient shows the lowest losses in the most important Reynolds number range $2 \cdot 10^5 < Re_2 < 7 \cdot 10^5$. For high turbulence levels no advantage in favor of the front-loaded cascade type T104 can be deduced.

Total Pressure Losses

The total pressure losses of the different cascades were determined from wake traverse measurements. Figure 18 shows the loss coefficient ζ_{V2} versus the deceleration rate w_{max}/w_{2th} for the three cascades, at design condition, and with the turbulence level as a parameter. The lowest losses are obtained for the aft-loaded cascade T106, at all turbulence levels; however, the advantage at the lowest turbulence level is small. The front-loaded type T104 shows a stronger influence of the turbulence level, this effect being directly connected to the boundary layer transition behaviour (see fig. 13). The second aft-loaded type T105 shows somewhat higher losses than the type T106 which is attributed to the stronger deceleration on the suction side. Thus, it is in particular this deceleration that has to be limited carefully to avoid increasing losses.

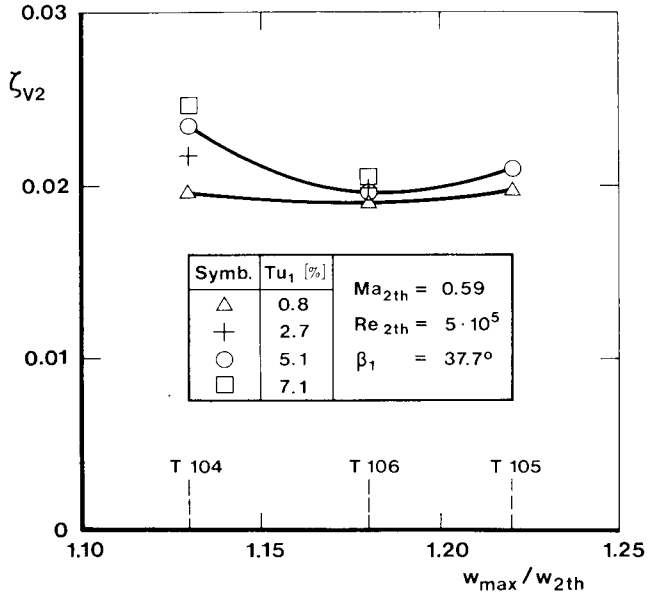

Figure 18: Effect of blade deceleration on measured loss coefficient at different turbulence levels

The stronger influence of the turbulence level on the front-loaded type T104 can also be seen to prevail in a wide Reynolds number range in comparison with the aft-loaded type T106 (figure 19). The behaviour of the loss coefficient confirms the boundary layer results for the suction side perfectly (see fig. 16). With increasing Reynolds number and increasing turbulence level additional losses are created due to the forward shift of transition.

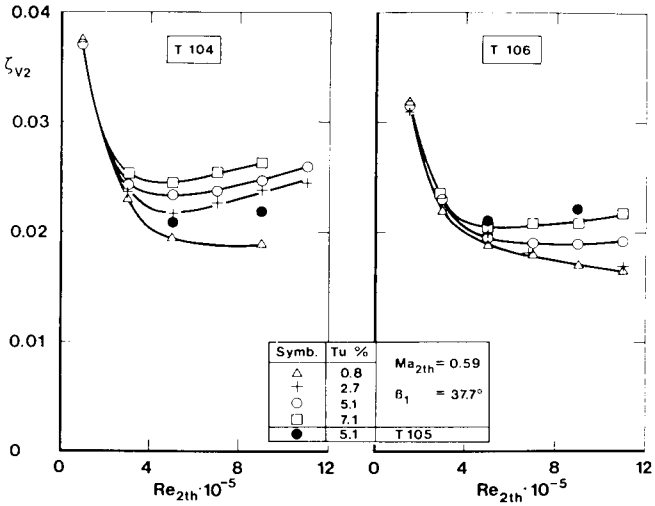

Figure 19: Effect of Reynolds number on measured loss coefficient at different turbulence levels

As discussed before, laminar separation bubbles are, in particular, responsible for the influence of the turbulence level on the total losses. To avoid the occurrence of laminar separation bubbles, several possible measures can be taken. One of these is to design a blade shape to have a slight adverse pressure gradient, which promotes transition without laminar separation. However, this can be done for one particular Reynolds number only. Since a

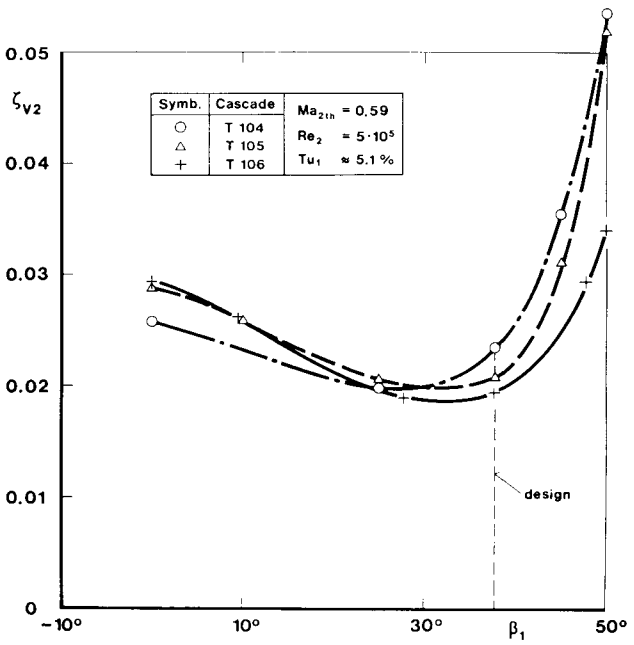

Figure 20: Effect of inlet angle on loss coefficient of different cascades

gas turbine blading has to work within a Reynolds number range, laminar separation bubbles will occur rather frequently. In order to avoid or to reduce these phenomena, mechanical or pneumatic turbulators can be used. As demonstrated e.g. by Hebbel [2] laminar separation bubbles can be made to disappear and consequently losses can be reduced by these devices. Another technique is the application of pneumatic turbulators as used successfully on single airfoils [26]. This principle was also tested with the present cascades by letting bleed air from the pressure to the suction side. Reductions of losses of about 10 % to 20 % can be achieved at Reynolds numbers $Re_2 < 3 \cdot 10^5$.

The results, discussed so far, pertained to design conditions. The three casdades were also investigated experimentally at different inlet angles (incidences) and Mach numbers. As shown in figure 20, for the most important turbulence level of about $Tu_1 = 5\,\%$, the aft-loaded type T106 preserves its advantage concerning loss behaviour almost over the whole incidence range. At positive incidences, $\beta_1 > 38^\circ$, a strong increase of the losses occurs especially on the front-loaded type T104.

With the design inlet angle kept constant, the influence of Mach number on the total pressure losses is plotted in figure 21, again for $Tu_1 = 5\,\%$. For subcritical Mach numbers, $Ma_{2th} < 0.85$, the aft-loaded type T106 produces the lowest losses. The comparison with the results for the second aft-loaded type T105 makes again quite clear that the deceleration on the suction surface has to be limited carefully. The front-loaded type T104 offers no advantage in the Mach number range of interest, $Ma_{2th} < 0.9$.

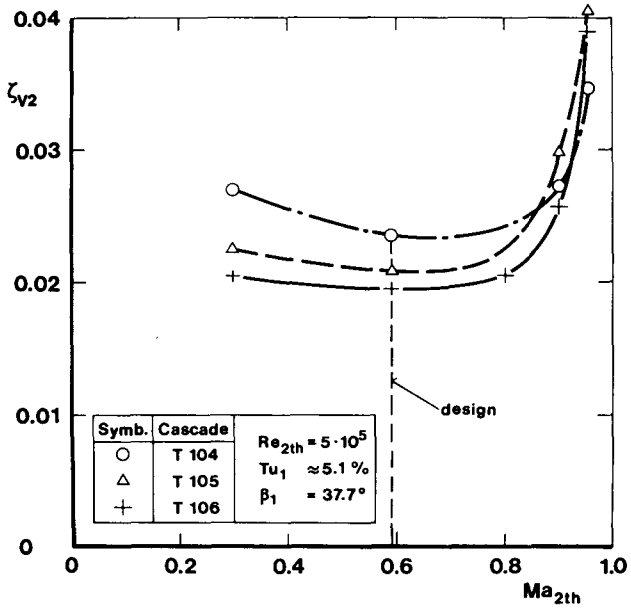

Figure 21: Effect of Mach number on loss coefficient of different cascades design inlet angle

CONCLUSIONS

The contribution describes theoretical and experimental investigations on the influence of free stream turbulence for three turbine cascades. These cascades were designed to have a prescribed velocity distribution and the same aerodynamic loading at a Mach number of $Ma_{2th} = 0.59$ and at a Reynolds number of $Re_2 = 5 \cdot 10^5$. Flow field calculations were performed using a time marching method to predict the final blade surface velocity distribution. In addition, a boundary layer integral method, including a transition criterion was applied to predict the influence of the degree of turbulence and pressure gradient on the momentum thickness along the blade suction surface. A series of experiments carried out in the High Speed Cascade Wind Tunnel of the DFVLR Braunschweig which, in general, confirm the theoretical results. Turbulence intensities up to $Tu \approx 8\,\%$ were generated. The investigations on one front-loaded type and on the two aft-loaded types of turbine cascades led to the following conclusions:

1. The type of the velocity distribution on the suction surface is of great importance in view of total pressure losses. The aft-loaded type with a carefully limited rearward deceleration yields low losses.
2. At realistic degrees of free stream turbulence, $Tu_1 > 2\,\%$, this aft-loaded velocity distribution leads to lower losses than the front-loaded velocity distribution. At the design Reynolds number $Re_2 = 5 \cdot 10^5$, a stronger influence of the free stream turbulence on the losses is observed for the front-loaded cascade.
3. At a given Reynolds number the laminar-to-turbulent boundary layer transition is, in particular, influenced by the occurrence of laminar separation bubbles. The streamwise location of the onset of transition as measured by different techniques could not be confirmed by the theoretical investigations due to the lack of more reliable transition criteria. In particular, at realistic turbine turbulence levels of $Tu_1 > 2\,\%$ transition onset is predicted by the theory to lie more upstream than was found from the experiments. Boundary layer transition appears to be always coupled with a laminar separation bubble in the Reynolds number range of interest.
4. The favourable characteristics of the aft-loaded cascade types found at design conditions continue to exist also at different incidences and at high subcritical exit Mach numbers.

ACKNOWLEDGEMENT

The work reported herein was supported within the framework of research programmes of the German "Bundesministerium der Verteidigung". The permission for publication is greatefully acknowledged. The authors are also indebted to T. Kotlarski, M. Hoeger and M. Meyer-Glitza for their help in carrying out these investigations. The assistance of P. Geisler, C. Giese, G. Laskowski, A. Rüberg is also appreciated.

REFERENCES

[1] Gostelow, J.P., Cascade Aerodynamics. Pergamon Press, 1984.

[2] Hebbel, H.H., Über den Einfluß der Machzahl und der Reynoldszahl auf die aerodynamischen Beiwerte von Turbinenschaufelgittern bei verschiedener Turbulenz der Strömung. Forschg. im Ing.-Wesen Vol. 30 (1964) No. 3, pp. 65-77.

[3] Kiock, R., Einfluß des Turbulenzgrads auf die aerodynamischen Eigenschaften von ebenen Verzögerungsgittern. Forschg. im Ing.-Wesen Vol. 39 (1973) No. 1, pp. 17-28.

[4] Kiock, R., Turbulence Downstream of Stationary and Rotating Cascades, ASME-paper 73-GT-80 (1973).

[5] Pfeil, H. und Pache, W., Messungen von Strömungsgrenzschichten unter Turbomaschinenbedingungen. Zeitschr. Flugwiss. Weltraumforsch. Vol. 1 (1977), No. 4, pp. 267-277.

[6] Abu-Ghannam, B.J. and Shaw, R., Natural transition of boundary layers - the effect of turbulence, pressure gradient and flow history. Jour. Mech. Eng. Sci. Vol. 22 (1980) No. 5, pp. 213-228.

[7] Sharma, O.P., Wells, R.A., Schlinker, R.H., Bailey, D.A., Boundary layer development on turbine airfoil suction surfaces. ASME-paper 81-GT-204 (1981).

[8] Blair, M.F., Influence of free-stream turbulence on boundary layer transition in favorable pressure gradients. Trans. ASME J. Eng. Pow. 104 (1982) No. 4, pp. 743-750.

[9] Rued, K., Wittig, S., Free-stream turbulence and pressure gradient effect on heat transfer and boundary layer development on highly cooled surfaces. ASME-paper 84-GT-180 (1984), to be published in J. Eng. Pow.

[10] Gaugler, R.E., A review and analysis of boundary layer transition data for turbine application. ASME-paper 85-GT-83 (1985).

[11] Eckardt, D., Weiß, H., Entwicklung der Niederdruckturbine für das Triebwerk PW 2037. Vortrag Nr. 84-109 b, DGLR-Jahrestagung Hamburg, 1-3 Okt. 1984.

[12] Schmidt, E., Computation of supercritical compressor and turbine cascades with a design method for transonic flows. ASME-paper 79-GT-30 (1979).

[13] Walz, A., Strömungs- und Temperaturgrenzschichten. Verlag G. Braun, Karlsruhe (1966).

[14] Granville, P.S., The calculation of viscous drag of bodies of revolution. Nave Depart. The David Taylor Mod. Basin Report No. 849 (1953), see also Schlichting, H. Grenzschichttheorie Verlag G. Braun, Karlsruhe, 8. Aufl. (1982).

[15] Seyb, N.J., The role of boundary layers in axial flow turbomachines and the prediction of their effects. AGARDograph No. 164 (1972), pp. 241-25.

[16] Dunham, J., Prediction of boundary layer transition on turbomachinery blades. AGARDograph No. 164 (1972), pp. 55-71.

[17] Hoheisel, H. and Kiock, R., Zwanzig Jahre Hochgeschwindigkeits-Gitterwindkanal des Instituts für Aerodynamik der DFVLR Braunschweig, Zeitschr. Flugwiss. Weltraumforsch. Vol. 1, No. 1 (1977), pp. 17-29.

[18] Kiock, R., Laskowski, G., Hoheisel, H., Die Erzeugung höherer Turbulenzgrade in der Meßstrecke des Hochgeschwindigkeits-Gitterwindkanals, Braunschweig, zur Simulation turbomaschinenähnlicher Bedingungen. DFVLR-FB 82-25 (1982), see also ESA-TT-815 (1983).

[19] Hoeger, M. and Hoheisel, H., On the accuracy of boundary layer measurements in cascades at high subsonic speeds. 7th Symposium on measuring techniques for transonic and supersonic flow in cascades and turbomachines. Aachen (1983). Mitt. 1/84 Inst. Strahlantriebe RWTH Aachen (1984).

[20] Hoheisel, H., Hoeger, M., Meyer, P., Koerber, G., A comparison of laser-Doppler anemometry and probe measurement within the boundary layer of an airfoil at subsonic flow. Second International Symposium on applications of laser anemometry to fluid mechanics, Lisbon, Portugal (1984).

[21] Oldfield, M.L.G., Kiock, R., Holmes, A.T., Graham, C.G., Boundary layer studies on highly loaded cascades using heated thin films and a traversing Probe. Trans. ASME J. Eng. Pow. Vol. 103 (Jan. 1981), pp. 237-246.

[22] Amecke, J., Anwendung der transsonischen Ähnlichkeitsregel auf die Strömung durch ebene Schaufelgitter., VDI-Forschungsheft 540 (1970), pp. 16-28.

[23] Lehthaus, F., Berechnung der transsonischen Strömung durch ebene Turbinengitter nach dem Zeit-Schritt-Verfahren. VDI-Forschungsheft 586 (1978).

[24] Hoheisel, H., Ergebnisse experimenteller Untersuchungen an Turbinengittern mit vorgegebener Druckverteilung. Vortrag DGLR-Symposium "Neue Beschaufelungskonzepte für axiale Turbomaschinen", Köln, Mai 1984.

[25] Hourmouziadis, J., Das Verhalten der Grenzschicht in Turbinengittern. Vortrag DGLR-Symposium "Neue Beschaufelungskonzepte für axiale Turbomaschinen", Köln, Mai 1984.

[26] Horstmann, K.H., Quast, A., Boermans, L.M.M., Pneumatic turbulators - a device for drag reduction at Reynolds numbers below $5 \cdot 10^6$. AGARD-CP-365 (1984), paper No. 20.